High field magneto-transport in two-dimensional electron gas $LaAlO_3/SrTiO_3$

Ming Yang', Kun Han, Olivier Torresin, Mathieu Pierre, Shengwei Zeng, Zhen Huang, T. V. Venkatesan, Michel Goiran, J. M. D. Coey, Ariando', and Walter Escoffier

Citation: Appl. Phys. Lett. **109**, 122106 (2016); doi: 10.1063/1.4963234
View online: http://dx.doi.org/10.1063/1.4963234
View Table of Contents: http://aip.scitation.org/toc/apl/109/12
Published by the American Institute of Physics

High field magneto-transport in two-dimensional electron gas $LaAlO_3/SrTiO_3$

Ming Yang,[1,a)] Kun Han,[2] Olivier Torresin,[1] Mathieu Pierre,[1] Shengwei Zeng,[2] Zhen Huang,[2] T. V. Venkatesan,[2] Michel Goiran,[1] J. M. D. Coey,[2,3] Ariando,[2,b)] and Walter Escoffier[1]
[1]*Laboratoire National des Champs Magnétiques Intenses (LNCMI-EMFL), CNRS-UGA-UPS-INSA, 143 Avenue de Rangueil, 31400 Toulouse, France*
[2]*Department of Physics and NUSNNI-Nanocore, National University of Singapore, Singapore 117411*
[3]*School of Physics and CRANN, Trinity College, Dublin 2, Ireland*

(Received 13 April 2016; accepted 10 September 2016; published online 23 September 2016)

The transport properties of the complex oxide $LaAlO_3/SrTiO_3$ interface are investigated under a high magnetic field (55 T). Small oscillations of the magnetoresistance with altered periodicity are observed when plotted versus the inverse magnetic field. We attribute this effect to Rashba spin-orbit coupling which remains consistent with large negative magnetoresistance when the field is parallel to the sample plane. A large inconsistency between the carrier density extracted from Shubnikov-de Haas analysis and from the Hall effect is explained by the contribution to transport of at least two bands with different mobilities. *Published by AIP Publishing.*
[http://dx.doi.org/10.1063/1.4963234]

Oxide interfaces constitute a rapidly developing field of research, with potential applications in electronics[1,2] or solar energy harvesting.[3] There is currently a focus on the band-insulators $LaAlO_3$ (LAO) and $SrTiO_3$ (STO), which host a conducting two-dimensional electron gas (2DEG) at their interface.[4] It is mainly believed to originate from the polar catastrophe,[5] which results in a charge transfer between the polar oxide [100] LAO and the nonpolar oxide [100] STO. This charge transfer prevents a divergence of the electrostatic potential associated with the intra-layer built-in electric field. Charge accumulation is therefore predicted at the interface with intriguing consequences such as magnetism[6] and superconductivity.[7] In LAO/STO heterostructures, symmetry-lowering at the interface raises the Ti t_{2g} band degeneracy so that the d_{xy} orbital is lower in energy than the d_{xz} and d_{yz} orbitals. Depending on the total two-dimensional carrier density, the band occupation and the spatial distribution of the carriers[8] are critical to envision band engineering for oxide electronics.[9,10] Experiments utilizing a capping layer,[11] tuning growth temperature,[12] or using ionic liquid gating[13] have allowed for a sufficiently high-mobility 2DEG to display Shubnikov-de Haas (SdH) oscillations under the magnetic field,[12,14,15] opening new perspectives for the investigation of the charge carriers' properties in relation to their band-structure. However, quantum transport studies remain scarce in the literature and the large variability in the results (originating from the large range of samples studied) does not yet offer a clear picture of electron transport in LAO/STO. In this context, we make use of very large magnetic field (55 T) to address the LAOSTO transport in low mobility samples. We interpret our experimental data by the presence of low and high mobility electrons both contributing to transport, and confirm the role of Rashba spin-orbit coupling.

Two samples named S_1 and S_2 were obtained by depositing 10 unit cells of LAO on the TiO_2-terminated (100)-oriented STO substrates using pulsed laser deposition (PLD).[16] Since both samples displayed similar results, we shall mainly discuss sample S_1 and make reference to sample S_2 only when relevant (full data for sample S_2 are available in the supplementary material). The LAO was grown at T = 740 °C in oxygen partial pressure of $P_{O_2} = 2 \times 10^{-3}$ Torr. During the deposition, *in-situ* reflection high energy electron diffraction (RHEED) was used to precisely control the layer-by-layer growth of LAO. The laser used in this work is a Lambda Physik Excimer KrF UV laser with the wavelength of 248 nm at a pulse rate of 1 Hz. After deposition, the samples were cooled down to room temperature at a rate of 15 °C/min in the same oxygen pressure as for the deposition. The samples were then annealed in a tube furnace at 550 °C for 1 h in air in order to remove the oxygen vacancies in the STO substrates introduced by high-energy plasma bombardment during the deposition.[17] The six-terminal Hall bar devices of width W = 50 μm and length L = 180 μm between the longitudinal probes were fabricated by conventional photolithography using amorphous AlN films as hard masks (see inset of Figure 1). The devices are electrically contacted using aluminum wedge bonding. The magnetoresistance and the Hall resistance were simultaneously measured during a pulse of magnetic field of up to 55 T with duration of 300 ms, using a DC current $i^{DC} = 10\,\mu$A. Small quantum oscillations with amplitude ~1% of the sheet resistance value were observed on top of a large monotonic background. To improve the signal-to-noise ratio and reveal the very faint amplitude of the oscillations, another experimental run was performed where the injected current is modulated at $f = 7$ kHz with RMS amplitude $i^{RMS} = 10\,\mu$A. The raw signal is later numerically demodulated, and the oscillating part is extracted after subtracting a smooth background. It is worth noting that the background signal (not shown here) is strongly distorted when compared to its DC counterpart (see supplementary material) and is discarded from analysis. Indeed, we believe that non-ohmic contacts result in signal attenuation when measured at high frequency under pulsed magnetic field, without much affecting the oscillating part. On the other hand, the monotonic signal is reliable when

a)ming.yang@lncmi.cnrs.fr
b)phyarian@nus.edu.sg

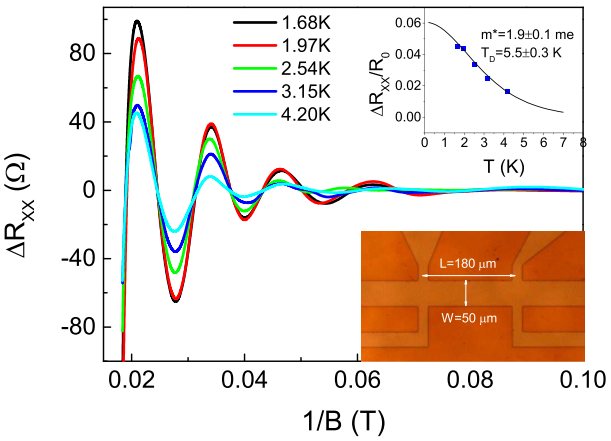

FIG. 1. Temperature dependence of the Shubnikov-de Haas oscillations in sample S_1 as a function of the inverse magnetic field after subtracting a smoothed background. Notice that the oscillation frequency is not exactly $1/B$-periodic but depends on magnetic field. The insets show the oscillations' amplitude fitted using the Lifshitz-Kosevich expression and a photo of the sample under optical microscope.

measured using DC current and will be addressed later. The samples can be rotated *in situ* with the current aligned along the magnetic field in the parallel configuration. The angle between the rotator and the magnetic field is precisely controlled using a pick-up coil. The typical sheet resistance of device S_1 is 74.5 kΩ/□ at 250 K and drops down to 417 Ω/□ at 4.2 K, in line with typical values in the literature.[16]

We first focus on the SdH oscillations displayed in Figure 1 and emphasize the imperfect periodicity of the oscillations when plotted as a function of inverse magnetic field. Indeed, careful experimental analysis indicates a period shift of $\sim 2\,\mathrm{T}^{-1}$ as the inverse magnetic field decreases. Traditionally, non-periodic oscillating features are interpreted in terms of the presence of several charge carriers, originating from different sub-bands, contributing to SdH oscillations with different periods. Usually, a Fourier transform of the raw signal usually allows extraction of the frequency peaks associated with the charge carriers. In the present case however, this procedure fails mainly because of the small number of oscillations and their *almost periodic* character. Furthermore, the general shape of the oscillations (the exponential-like envelope) is suggestive of a single band contribution. Although the multi-band scenario cannot be totally excluded, we focus here on an alternative explanation involving spin-orbit coupling. Since the effective mass m^* enters in the equations of this model, we first estimate this parameter (as well as the quantum mobility $\mu_q = e\tau_q/m^*$) by studying the temperature dependence of the amplitude of the SdH oscillations using the Lifshitz-Kosevich (LK) equation below.

$$\Delta R_{xx}(T) = 4R_0 \times \exp(-\beta T_D) \times \frac{\beta T}{\sinh(\beta T)}. \qquad (1)$$

Here, ΔR_{xx} is the oscillation amplitude at a given magnetic field B, R_0 is the non-oscillatory component of the magnetoresistance, $\beta = \frac{2\pi^2 k_B m^*}{\hbar e B}$ is a prefactor while $T_D = \hbar/2\pi k_B \tau_q$ and τ_q are the Dingle temperature and the quantum scattering time, respectively. The best fit of $\Delta R_{xx}(T)$ is obtained with parameters $m^* = 1.9 \pm 0.1 \times m_e$ (where $m_e = 9.1 \times 10^{-31}$ kg is the bare electron mass) and $\mu_q = 203 \pm 15\,\mathrm{cm}^2/\mathrm{Vs}$ (see inset of Figure 1). Several authors[15,18,19] have considered the influence of the Rashba spin-orbit coupling in the electronic properties of LAO/STO interface, arising from the interfacial breaking of inversion symmetry. In the presence of a strong perpendicular magnetic field, the usual Landau Level (LL) spectrum is modified and reads

$$\begin{cases} E_{(N=0)} = \kappa_{(B)} \\ E^{\pm}_{(N>0)} = N\hbar\omega_c \mp \sqrt{\kappa^2_{(B)} + N\dfrac{2\alpha^2 eB}{\hbar}}, \end{cases} \qquad (2)$$

where $\kappa_{(B)} = \frac{1}{2}\hbar\omega_c - \frac{1}{2}g^*\mu_B B$, N is a positive integer, $\omega_c = \frac{eB}{m^*}$ is the cyclotron pulsation, g^* is the spin-orbit enhanced Lande factor and α is the strength of the spin-orbit coupling. Following the lines of Ref. 15, the Fermi energy is computed by equating the total density of states at a given magnetic field to the fixed carrier density of the system. Considering the field-dependent orbital degeneracy of the Landau Levels (LLs) and their spectrum given by Equation (2), the Fermi energy actually evolves non-monotonically within the LL band-structure. As the Fermi energy alternatively crosses a LL or remains in between two LLs, the magnetoresistance oscillates, respectively, above or below the mean resistance value, giving rise to SdH oscillations. LL broadening is taken into account using a Gaussian line shape with $\sqrt{B}$ variance. The B-rising amplitude of the oscillations is finally adjusted using an exponential function. Figure 2 shows the best fit obtained using this procedure for sample S_1 and S_2, from which we extract the free parameters n, g^* and α, m^* is constrained to be $1.9m_e$ as found earlier (see inset of Figure 1). Despite an inevitable uncertainly in the determination of the Rashba constant and g-factor (due to the limited number of oscillations), they both fall in the range of reported values in the literature.[15,18] We would like to emphasis that the set of parameters $\{\alpha = 5.45 \times 10^{-12}\,\mathrm{eVm},\ g^* = 5\}$ is unique for each sample provided the carrier density remains close to the one computed using the usual Onsager relation $n = (ed_s)/(hT_{SdH})$. Here, $d_s = 2$ is the spin degeneracy and T_{SdH} is the mean period of the oscillations plotted against inverse magnetic field (neglecting the imperfect periodicity

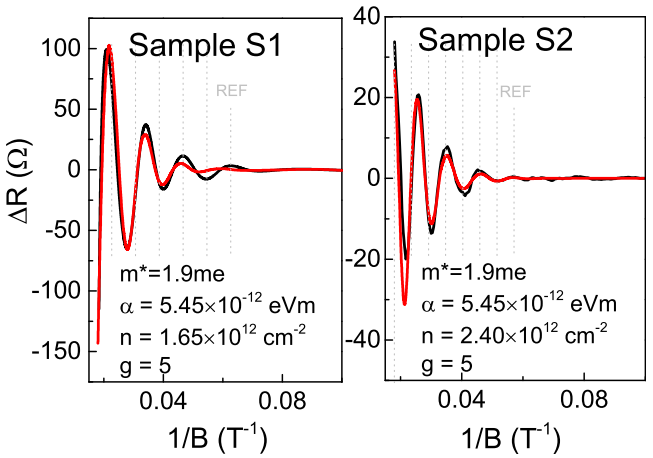

FIG. 2. Fit (red line) of SdH oscillations for samples S_1 and S_2 using Equation (2) in the presence of spin-orbit coupling. The black line corresponds to the experimental data. Vertical dotted lines are guide for eyes. "REF" stands for the arbitrary reference for the 1/B periodicity.

of the SdH oscillations). The obtained carrier density $n \sim 10^{12}\,\mathrm{cm}^{-2}$ is of the same order of magnitude as found in other studies of similar samples,[13,20] but remains almost two orders of magnitude lower than the predictions of the polar catastrophe model. Furthermore, it is inconsistent with the value extracted from the linear Hall effect $n_H = 1.48 \times 10^{13}\,\mathrm{cm}^{-2}$ shown in Figure 3. This discrepancy is actually a long standing issue and several interpretations have been proposed. First, the presence of valley degeneracy has been considered in the literature[20] and would provide a natural explanation involving a complex band-structure. However the non-integer ratio n_H/n (Ref. 21) in the present study does not favor this hypothesis. It is worth noting, in addition, that different ratios ranging from roughly 2 to 5 have been reported in the literature[12,14,20,22] and are therefore linked to sample's growth conditions rather than to a universal band-structure characteristic. The difference between n_H and n can be reconciled assuming one or more additional conduction channels which do not contribute to SdH oscillations. In this framework, the Hall resistance can be approached using a two-fluid model, where one type of carriers are characterized by carrier density n_1 and mobility $\mu_{t,1}$ while the other type is defined by n_2 and $\mu_{t,2}$. We assume that both carrier densities n1 and n2 relate to 2DEG, and that the lower mobility fluid can include several indistinguishable sub-bands. We have

$$R_{xy}(B) = \frac{B}{e} \times \frac{\left(n_1\mu_{t,1}^2 + n_2\mu_{t,2}^2\right) + \left(\mu_{t,1}\mu_{t,2}B\right)^2(n_1+n_2)}{\left(n_1\mu_{t,1} + n_2\mu_{t,2}\right)^2 + \left(\mu_{t,1}\mu_{t,2}B\right)^2(n_1+n_2)^2},$$
$$R_{(B=0)} = \frac{L}{W} \times \left(e \cdot n_1\mu_{t,1} + e \cdot n_2\mu_{t,2}\right)^{-1}. \quad (3)$$

Note that $\mu_{t,i}$ $(i = 1, 2)$ stands for the transport mobility, not the quantum mobility μ_q defined earlier. It is worth noting that the magnetic field evolution of $R_{xx}(B)$ is discarded from this analysis since a negative magnetoresistance contribution (related to spin-orbit coupling) is not captured by this simple model. Only the zero-field sample resistance $R_{(B=0)}$ is therefore considered. We assume that both carrier densities n_1 and n_2 relate to 2DEG. When $\mu_{t,1} \neq \mu_{t,2}$, the two carrier model yields a non-linear Hall effect, contrary to the experimental finding where the linearity of $R_{xy}(B)$ is established for the full magnetic field range [0–55 T], but the linear B behaviour of the Hall resistance is progressively restored when $\mu_{t,1}/\mu_{t,2}$ approaches unity. Setting $n_1 = 1.65 \times 10^{12}\,\mathrm{cm}^{-2}$, the value derived from the SdH oscillations, the best fit for the Hall resistance is obtained for $n_2 = 1.24 \times 10^{13}\,\mathrm{cm}^{-2}$, $\mu_{t,2} = 948\,\mathrm{cm}^2/\mathrm{Vs}$, and $\mu_{t,1} = 1872\,\mathrm{cm}^2/\mathrm{Vs}$ for sample S_1.

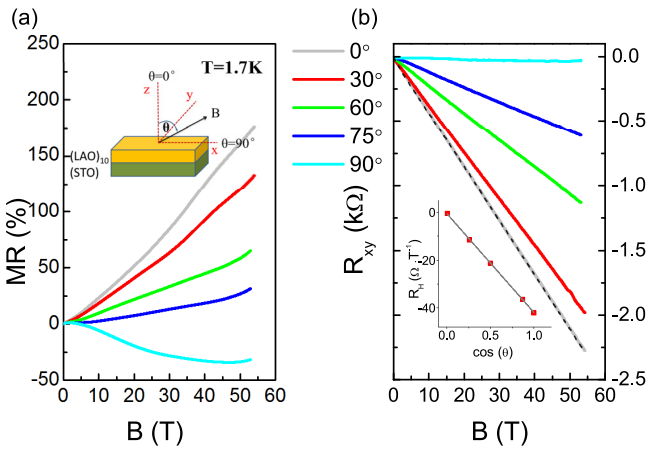

FIG. 3. Longitudinal magnetoresistance (a) and Hall resistance (b) at T = 1.7 K as a function of the tilt angle between the sample's plane and the magnetic field for sample S_1. Inset of (b) displays the linear variation of the Hall coefficient versus the cosine of the tilt angle. The dashed line in panel (b) is the fit of $R_{xy}(B)$ using the two-fluid model with $n_1 = 1.65 \times 10^{12}\,\mathrm{cm}^{-2}$, $\mu_{t,1} = 1872\,\mathrm{cm}^2/\mathrm{Vs}$, $n_2 = 1.24 \times 10^{13}\,\mathrm{cm}^{-2}$, and $\mu_{t,2} = 948\,\mathrm{cm}^2/\mathrm{Vs}$.

Based on the above analysis, we now would like to comment on the origin and transport properties of the two electron fluids. The SdH oscillations originate from heavy-mass carriers ($m^* = 1.9m_e$) which are probably derived from d_{xz} and d_{yz} orbitals extending deep in the STO side of the interface.[15] These minority carriers have a density of the order of $\sim 10^{12}\,\mathrm{cm}^{-2}$ and a fairly high mobility of a few thousands $\mathrm{cm}^2/\mathrm{Vs}$. Moreover, their quantum mobility is much lower than their transport mobility by roughly a factor 9, suggesting that long-range scattering is dominant.[23] Indeed, the quantum mobility is linked to the averaged elastic scattering time whereas the transport mobility is determined by the total scattering weighted by the scattering angle. When long-range scattering is dominant and account for isotropic diffusion processes, the quantum mobility is smaller than its transport counterpart. The presence of charged O^{2-} vacancies close to the interface or in the LAO layer[24] provides strong support for this hypothesis, although their influence is certainly reduced by screening as the charge distribution extends deeper in the STO layer. On the other hand, we attribute the non-oscillatory part of the magnetoresistance to charge carriers lying in the lowest energy sub-band derived from the d_{xy} orbitals. Such carriers are concentrated within a few unit cells of the interface between LAO and STO and certainly experience strong scattering from ionic inter-diffusion and interface reconstruction. Consequently, these charge carriers should display low mobility and are not expected to contribute to SdH oscillations. It is worth noting that even if the two fluid model captures the essence of the underlying physics, it is certainly oversimplified to account for a progressive charge distribution from the interface to deep inside the STO layer, involving a continuous crossover from low to high mobility carriers.

The magnetic field dependence of the SdH oscillation frequency deserves further attention. The apparent departure from $1/B$ periodic behaviour was already observed in Ref. 25. The authors interpreted this result as a change of carrier density with increasing magnetic field, which would be of up to 1250% over the full magnetic field range of the present study. However this hypothesis is inconsistent with the results of the two-fluid model (see the supplementary material) and a more natural explanation involving Rashba spin-orbit coupling is favored. Indeed, the SdH oscillations can be pretty well fitted within this framework for both samples and the extracted free parameters (namely, the carrier density, g^*-factor and spin-orbit strength) are in line with values recently reported in a similar system.[15] The presence of Rashba spin-orbit coupling is also consistent with the negative magnetoresistance of the order of 35% when the magnetic field is parallel to the plane of the sample (see Figure 3). The interplay between electron scattering and spin-orbit coupling in the framework of the

Boltzmann formalism applicable to disordered samples can yield a giant negative magnetoresistance[26] as experimentally observed. The growth conditions certainly have a large impact on the sample's magnetoresistance response, so that a direct comparison of our data with the results of Ref. 26 is impractical, however the magnitude of the magnetoresistance and the saturation field, which strongly depends on the carrier density, are in qualitative agreement. An alternative would be to attribute the negative and saturating magnetoresistance to scattering of charge carriers by localized magnetic moments. As the magnetic field increases, spin-flip scattering is progressively reduced and translates in to a decrease of resistance. According to this hypothesis, saturation of the magnetoresistance is roughly expected when the Zeeman energy $\epsilon_Z = g^* \mu_B B_{\|}^*$ matches the spin-orbit coupling energy $\epsilon_{SO} = \frac{m^* \alpha^2}{2\hbar^2}$. Using the parameters derived above, the extracted characteristic field is one order of magnitude lower than the experimental one, which invalidates the hypothesis. Furthermore, the persistence of negative magnetoresistance at elevated temperature (20 K) (see the supplementary material) is not consistent with the Kondo interpretation.

To conclude, our experimental results in high magnetic field are consistent with recent published studies insofar as they support the presence of at least two conduction channels with different mobility. The high mobility carriers, with twice the bare electron mass, are located deep in the STO material but remain sensitive to charge impurities at the surface. The presence of O^{2-} vacancies is at the origin of a long-range disorder, which translates into a large difference between the Drude and Dingle scattering times. The mobile electron carriers are studied through SdH oscillations with reproducible deviations from $1/B$ periodicity. This effect is interpreted as a consequence of Rashba spin-orbit coupling, consistent with the large negative, saturating magnetoresistance when the field is applied parallel to the sample plane. On the other hand, the low mobility carriers are located close the LAO/STO interface and experience strong scattering, so that the corresponding SdH oscillations remain out of experimental reach even in magnetic fields as high as 55 T. Their contribution is visible in the linear Hall effect, with carrier density roughly one order of magnitude higher than the mobile electrons. In order to validate these conclusions, a higher magnetic field study with varying carrier concentration would be required. It will be part of our future study.

See supplementary material for more information, which includes the magnetic transport measurement detail, the two fluid model with field dependent carrier density, the negative MR in parallel field at 20 K, the fittings of SdHO of Rashba, and the substraction of the SdH oscillations.

Sample fabrication by PLD was carried out at National University of Singapore. Low temperature and high magnetic field measurements were performed at LNCMI under the EMFL proposal TSC16-213. This work was partly supported by the scholarship from China Scholarship Council (CSC) under the Grant CSC No. 201404490072 and the National University of Singapore (NUS) Academic Research Fund (AcRF Tier 1 Grant Nos. R-144-000-346-112 and R-144-000-364-112).

[1]J. Mannhart and D. Schlom, Science (N. Y.) **327**, 1607 (2010).
[2]H. Hwang, Y. Iwasa, M. Kawasaki, B. Keimer, N. Nagaosa, and Y. Tokura, Nat. Mater. **11**, 103 (2012).
[3]E. Assmann, P. Blaha, R. Laskowski, K. Held, S. Okamoto, and G. Sangiovanni, Phys. Rev. Lett. **110**, 078701 (2013).
[4]A. Ohtomo and H. Hwang, Nature **427**, 423 (2004).
[5]J. Mannhart, D. Blank, H. Hwang, A. Millis, and J. Triscone, MRS Bull. **33**, 1027 (2008).
[6]A. Brinkman, M. Huijben, M. van Zalk, J. Huijben, U. Zeitler, J. Maan, W. van der Wiel, G. Rijnders, D. Blank, and H. Hilgenkamp, Nat. Mater. **6**, 493 (2007).
[7]N. Reyren, S. Thiel, A. Caviglia, L. Kourkoutis, G. Hammerl, C. Richter, C. Schneider, T. Kopp, A. S. Rüetschi, D. Jaccard, M. Gabay, D. Muller, J. M. Triscone, and J. Mannhart, Science (N. Y.) **317**, 1196 (2007).
[8]Z. Huang, X. R. Wang, Z. Q. Liu, W. M. Lü, S. W. Zeng, A. Annadi, W. L. Tan, X. P. Qiu, Y. L. Zhao, M. Salluzzo, J. M. D. Coey, T. Venkatesan, and Ariando, Phys. Rev. B **88**, 161107 (2013).
[9]B. Forg, C. Richter, and J. Mannhart, Appl. Phys. Lett. **100**, 053506 (2012).
[10]D. Stornaiuolo, C. Cantoni, G. M. D. Luca, R. D. Capua, E. D. Gennaro, G. Ghiringhelli, B. Jouault, D. Marrè, D. Massarotti, F. M. Granozio, I. Pallecchi, C. Piamonteze, S. Rusponi, F. Tafuri, and M. Salluzzo, Nat. Mater. **15**, 278 (2015).
[11]M. Huijben, G. Koster, M. K. Kruize, S. Wenderich, J. Verbeeck, S. Bals, E. Slooten, B. Shi, H. J. A. Molegraaf, J. E. Kleibeuker, S. van Aert, J. B. Goedkoop, A. Brinkman, D. H. A. Blank, M. S. Golden, G. van Tendeloo, H. Hilgenkamp, and G. Rijnders, Adv. Funct. Mater. **23**, 5240 (2013).
[12]A. D. Caviglia, S. Gariglio, C. Cancellieri, B. Sacépé, A. Fête, N. Reyren, M. Gabay, A. F. Morpurgo, and J. Triscone, Phys. Rev. Lett. **105**, 236802 (2010).
[13]S. Zeng, W. Lü, Z. Huang, Z. Liu, K. Han, K. Gopinadhan, C. Li, R. Guo, W. Zhou, H. H. Ma, L. Jian, T. Venkatesan, and Ariando, ACS Nano **10**, 4532 (2016).
[14]A. McCollam, S. Wenderich, M. K. Kruize, V. K. Guduru, H. J. A. Molegraaf, M. Huijben, G. Koster, D. H. A. Blank, G. Rijnders, A. Brinkman, H. Hilgenkamp, U. Zeitler, and J. C. Maan, APL Mater. **2**, 022102 (2014).
[15]A. Fête, S. Gariglio, C. Berthod, D. Li, D. Stornaiuolo, M. Gabay, and J. Triscone, New J. Phys. **16**, 112002 (2014).
[16]Ariando, X. Wang, G. Baskaran, Z. Liu, J. Huijben, J. Yi, A. Annadi, A. Barman, A. Rusydi, S. Dhar, Y. Feng, J. Ding, H. Hilgenkamp, and T. Venkatesan, Nat. Commun. **2**, 188 (2011).
[17]Z. Q. Liu, C. J. Li, W. M. Lü, X. H. Huang, Z. Huang, S. W. Zeng, X. P. Qiu, L. S. Huang, A. Annadi, J. S. Chen, J. M. D. Coey, T. Venkatesan, and Ariando, Phys. Rev. X **3**, 021010 (2013).
[18]A. D. Caviglia, M. Gabay, S. Gariglio, N. Reyren, C. Cancellieri, and J. M. Triscone, Phys. Rev. Lett. **104**, 126803 (2010).
[19]A. Fête, S. Gariglio, A. D. Caviglia, J. Triscone, and M. Gabay, Phys. Rev. B **86**, 201105 (2012).
[20]M. B. Shalom, A. Ron, A. Palevski, and Y. Dagan, Phys. Rev. Lett. **105**, 206401 (2010).
[21]For sample S1, $n_H = 1.48 \times 10^{13}\,\mathrm{cm}^{-2}$ and $1.54 \times 10^{12}\,\mathrm{cm}^{-2} < n < 3.71 \times 10^{12}\,\mathrm{cm}^{-2}$ depending on B, so that $3.98 < \frac{n_H}{n} < 9.61$. For sample S2, $\mathrm{n_H} = 2.31 \times 1013\,\mathrm{cm}^{-2}$ and $3.13 \times 1012\,\mathrm{cm}^{-2} < \mathrm{n} < 4.97 \times 1012\,\mathrm{cm}^{-2}$ depending on B so that $4.65 < \frac{n_H}{n} < 7.38$.
[22]Y. Xie, C. Bell, M. Kim, H. Inoue, Y. Hikita, and H. Y. Hwang, Solid State Commun. **197**, 25 (2014).
[23]P. Coleridge, Phys. Rev. B: Condens. Matter **44**, 3793 (1991).
[24]A. P. Petrovic, A. Paré, T. R. Paudel, K. Lee, S. Holmes, C. H. W. Barnes, A. David, T. Wu, E. Y. Tsymbal, and C. Panagopoulos, Sci. Rep. **4**, 5338 (2014).
[25]B. Jalan, S. Stemmer, S. Mack, and J. S. Allen, Phys. Rev. B **82**, 081103 (2010).
[26]M. Diez, A. Monteiro, G. Mattoni, E. Cobanera, T. Hyart, E. Mulazimoglu, N. Bovenzi, C. Beenakker, and A. Caviglia, Phys. Rev. Lett. **115**, 016803 (2015).